

Low-temperature ordering in a substitutional alloy with injecting nonequilibrium vacancies: The FePt case

N. I. Polushkin

Institute for Physics of Microstructures of RAS, 603807, Nizhny Novgorod, Russia

Achieving the compositionally ordered state in a substitutional alloy of two or more species can often be even critical for improving its functional properties. To produce a highly ordered alloy, a longtime high-temperature (up to $T \sim 1000$ K) treatment of the alloy is typically necessary because of insufficient vacancy concentration (c_v) and their mobility. However, such processing affects the morphology and complicates the technology of functional alloys. We show theoretically that the ordering in the practically important FePt system ($\text{Fe}_x\text{Pt}_{1-x}$ with x being close to 0.5) is already achievable at $T \sim 450$ K for reasonable times $t < 10^3$ s due to frozen nonequilibrium vacancies. Our simulation is based on the Dienes equation for relaxation of the long-range order parameter (S), with taking additionally into account that the ordering kinetics in the alloy is mediated by vacancies. Importantly, the results of such simulation are in good agreement with previous experimental data on the ordering kinetics. We also find that nanosecond laser pulses can be employed to achieve a sufficient level of $c_v \sim 10^{-5}$ for effective low-temperature ordering.

Keywords: long-range order parameter, order-disorder transformations, nonequilibrium vacancy, substitutional alloy, laser quenching

I. INTRODUCTION

Typically, a substitutional alloy prepared, for example, in its thin-film form by sputtering onto a cold substrate gets its disordered state, e.g., Refs. [1-8]. If the energy of mixing is negative, i.e., $|V_{ij}| > |V_{ii(jj)}|$, where V_{ij} , V_{ii} , and V_{jj} are the interatomic potentials in a binary i-j alloy, it has a tendency to compositionally order via vacancy migration [9-16] at temperatures T lower than the critical temperature T_c for the order-disorder phase transition [17, 18]. Because of insufficient vacancy concentration, c_v , in the atomic lattice one should employ high enough annealing temperatures $T \sim 700-1000$ K $< T_c$, in order to activate the ordering process for long enough times [1-8]. However, a longtime high-temperature process would be undesirable in view of the compatibility for a practical device fabrication.

An example of functional alloys with order – disorder transformations is the $\text{Fe}_x\text{Pt}_{1-x}$ system, where $x \sim 0.5$ (FePt) [1-8, 11, 14, 19-26], which is crystallized in a face-centered cubic (fcc) lattice with the lattice constant of $a = 0.381$ nm in the disordered alloy. Obtaining the ordered $L1_0$ state in the FePt lattice is of great practical importance [19-23]. As the melting temperature $T_m \approx 1800$ K is higher than $T_c \approx 1600$ K in FePt [27], the phase transition occurs in the solid state. To optimize the annealing temperature and timescale regimes for the ordering process, both experimental [1-8] and theoretical [25] efforts were previously taken with FePt thin films. For example, it was demonstrated that extensive ordering with formation of the ordered $L1_0$ -FePt state occurs at

$T \sim 800$ K for a time $t \sim 10^2$ s [1, 5]. The ordering timescale can be shortened even to milliseconds [6, 7] at expense of annealing temperature elevation to $T \sim 1000$ K [7]. To provide the ordering at lower T , different technological tricks were employed, e.g., fabrication of multilayers (alternate deposition of Fe and Pt monolayers) [1, 3, 5, 7], stress-promoted $L1_0$ ordering transformations [4], adding a third element into FePt [2, 21, 22].

Here, we show theoretically that the annealing temperature needed for long-range compositional ordering in FePt alloys occurring for reasonable times, $t < 10^4$ s, can be lowered even to $T \sim 450$ K. Such effective low-temperature ordering is conceivable under the two conditions as follows: (1) The initial concentration of vacancies, $c_v(0)$, in the alloy should be high enough, while (2) T should be low enough, so that vacancies could not migrate and annihilate at boundaries of the alloy (crystallites). The simulation we have done is based on the Dienes equation for relaxation of the long-range order parameter S [28]. In addition, we redefine the rate constants for order-disorder transformations to be proportional to the quantity of c_v which is time-dependent. To derive $c_v(t)$, we use the linear differential equation of the Bloch type [29]. Qualitatively, it is obvious that the higher $c_v(t) \sim c_v(0)$ (when vacancies are frozen at low T and not able to migrate and annihilate), the larger the ordering rate. However, there is a task of quantifying the effect of $c_v(0)$ on the ordering kinetics. Indeed, even if $c_v(t) \sim c_v(0)$ persists at high enough level, the ordering process can be not activated at too low T .

The paper is organized in the following way. First, in the methodological section we describe (A) the

approaches we use to simulate the ordering kinetics as well as the temporal evolution of the vacancy concentration. We also give (B) a description of material parameters, which are important for quantifying the effect of vacancy concentration on the ordering kinetics. Obtained results and their discussion are divided into the following sections: (C) Comparison of the simulation results to experimental data reported earlier by different authors; (D) Evaluation of the effect of initial vacancy concentration, $c_v(0)$, on the ordering rate at low temperatures and (E) the proposal how to increase $c_v(0)$ for achieving effective low-temperature ordering.

II. METHODOLOGY

A. Ordering kinetics

Figure 1 (a) illustrates a scenario for a diffusion act via the vacancy mechanism in the fcc lattice of a substitutional i-j alloy with negative energy of mixing, which increases its order degree. In the beginning, a jump of a “wrong” j^α atom of the component j occurs into its correct position on the β -sublattice occupied initially by a vacancy (empty box), and then a “wrong” atom i^β of the component i jumps into the released site on the α -sublattice. The ordered $L1_0$ state can be formed in the FePt lattice due to such ordering events, whose number per unit of time exceeds the number of disordering events if $T < T_c$.

For previous decades there were proposed various approaches to modeling the ordering kinetics, e.g., Refs. [9, 10, 12, 16, 28]. A relatively simple

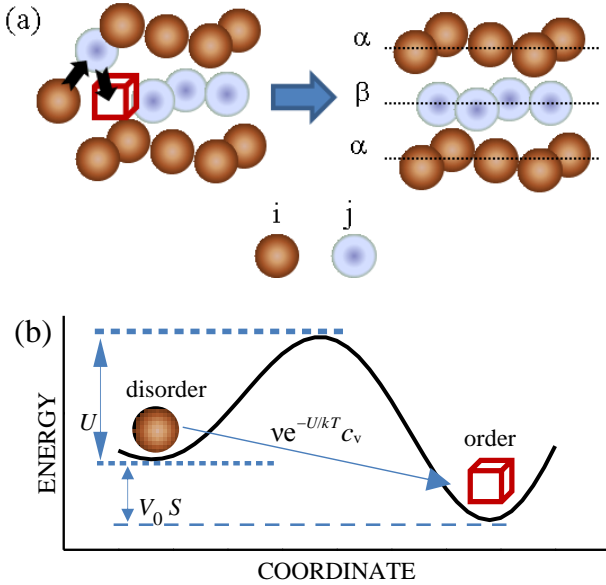


Fig.1. (a) Possible scenario for an ordering event via migration of a vacancy (empty box) in a substitutional alloy i-j. (b) The energy diagram for compositional order-disorder phase transformations at $T < T_c$.

formalism to describe the process has been developed by Dienes [28], who simulated compositional ordering/ disordering upon the basis of the chemical balance equation for the change rate of “wrong” atoms, namely

$$\frac{d(W/N)}{dt} = -K_1 \left(\frac{W}{N}\right)^2 + K_2 \left(x - \frac{W}{N}\right) \left(1 - x - \frac{W}{N}\right), \quad (1)$$

where W/N is the fraction of “wrong” atoms in the lattice and $K_{1(2)}$ is the rate constant for the ordering (disordering) process. Eq. (1) does not take explicitly into account the vacancy concentration in the lattice and can be used under the condition that $c_v \ll x \sim 0.5$. The equilibrium (thermal) vacancy concentration is given by

$$c_{eq}(T) = \exp\left[\frac{s_v}{k}\right] \times \exp\left[-\frac{E_v}{kT}\right] \quad (2)$$

where s_v and E_v are the vacancy formation entropy and energy, respectively, and k is the Boltzmann constant.

According to Dienes presentation, the rate constants are as follows:

$$K_1 = \nu \exp\left[-\frac{U}{kT}\right], K_2 = \nu \exp\left[-\frac{U + V_0 S}{kT}\right], \quad (3)$$

where $V_0 = |V_{ij} - 1/2(V_{ii} + V_{jj})| = kT_c/\Gamma$ [17, 18], $\Gamma = x(1-x)$, S is the long-range order parameter which relates to the number of “wrong” atoms as $W/N = \Gamma(1-S)$ [28], $\nu = D_0/a^2$ is the vibration frequency, and D_0 is the prefactor in the Arrhenius law for atomic diffusion, i.e., $D = D_0 \exp(-E/kT)$ with E being the activation energy. The physical meaning of U and $V_0 S$ is illustrated in Fig. 1 (b), which schematically presents the barriers for ordering and disordering events at $T < T_c$.

As for the $K_{1(2)}$ coefficients, these quantities represent the atomic/vacancy diffusivity D_m . In a substitutional alloy, where diffusion occurs through vacancies, K_1 and K_2 have to be redefined to linearly depend on c_v . As a result, Eq. (1) can be rewritten as follows:

$$\frac{dS}{dt} = \frac{D_m}{a^2} c_v(t) \left\{ \Gamma(1-S)^2 \left(\exp\left[\frac{V_0 S}{kT}\right] - 1 \right) - S \right\}, \quad (4)$$

where $D_m = D_0 \exp(-E_m/kT)$ and $E_m = U + V_0 S$ is the migration barrier. It is also assumed that $c_v(t)$ is governed by a linear differential equation which describes the vacancy relaxation, namely [29]

$$\frac{dc_v}{dt} = \frac{c_{eq} - c_v}{\tau}, \quad (5)$$

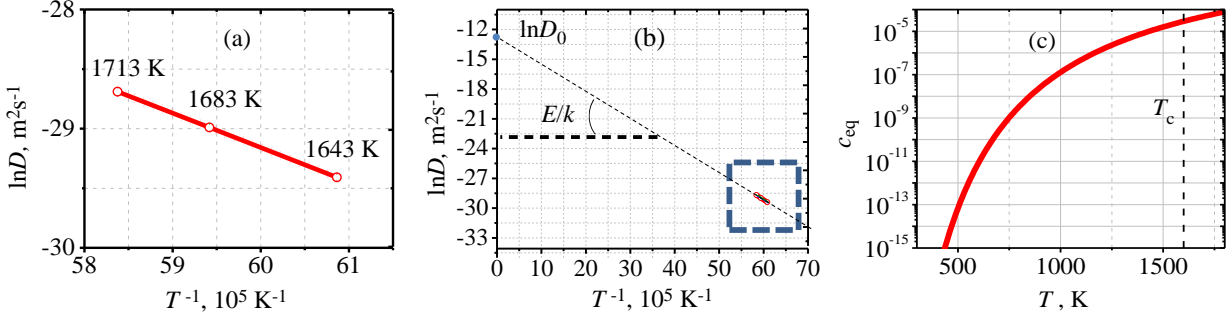


Fig.2. (a) Experimental $D(T)$ dependence in FePt taken from Ref. [26]. (b) Finding D_0 and E from obtained D . (c) c_{eq} versus T in FePt.

where $\tau=L^2/D_m$ is the characteristic time for vacancy annihilation at a boundary of the alloy or crystallite, and L is the linear size of the sample (film thickness) or crystallite diameter. The solution of Eq. (5) is

$$c_v(t) = \frac{1}{M(t)} [c_v(0) + (1/\tau_0) \int_0^t M(t)\eta(t) dt], \quad (6)$$

where $M(t) = \exp[(1/\tau_0) \int_0^t \exp[-E_m/kT(t)] dt]$, $\tau_0=L^2/D_0$, and $\eta(t)=c_{eq}[T(t)] \times \exp[-E_m/kT(t)]$. In the isothermal regime, the solution (6) simplifies to be

$$c_v(t) = c_v(0) \exp(-t/\tau) + c_{eq}(1 - \exp(-t/\tau)). \quad (7)$$

Thus, the solution of Eq. (5) reflects the fact that the factor of $c_v(0)$ contributes to $c_v(t)$ only if $t << \tau$ for migration and annihilation at boundaries of the alloy or crystallites. It is also obvious that $c_v(t) \rightarrow c_{eq}$ in the other limit ($t \gg \tau$).

B. Determination of material parameters

To quantify the effect of $c_v(t)$, there is a necessity to determine the material parameters in Eqs. (1-7), i.e., D_0 , E_m , E_v , and $c_{eq}(T)$. Figure 2 (a-b) shows the experimental $D(T)$ dependence in FePt bulk, which was obtained in Ref. [26]. It is important to note that diffusion processes were studied by authors of Ref. [30] at such high temperatures $T > T_c$ that the behavior of the component concentration was obeyed the Fick's law under the approximation of ideal solution. Thus, it was possible to measure atomic diffusivities D with the help of the Boltzmann-Matano method [30] which is typically used to investigate diffusion processes in metallurgical systems.

The $D(T)$ dependence shown in Fig. 2 (a) enables us to determine the prefactor D_0 in the Arrhenius law as well as the diffusion activation energy $E=E_m+E_v$ from the following relation:

$$\ln D = \ln D_0 - (E/k)T^{-1}, \quad (8)$$

which is illustrated in Fig. 2 (b). As a result, one gets that $E=2.5 \pm 0.2$ eV and $D_0=(2.5 \pm 0.5) \times 10^{-6}$ m²/s. The

quantity of E_v can be taken from the simulations of this parameter in Ref. [14], where it was shown that E_v depends on T over a broad temperature range (600–1800 K) and can be approximated as

$$E_v = 0.000295 \times T (\text{eV K}^{-1}) + 1.245. \quad (9)$$

Then, the quantity of E_m can be found by subtraction of E_v from E which, in turn, can be determined from Eq. (8). Finally, by taking into account Eq. (9) for E_v and that $s_v/k=2$ [15], one can find $c_{eq}(T)$ in FePt, which is plotted in Fig. 2 (c).

III. RESULTS AND DISCUSSION

C. Comparison to the experiments

Firstly, we compared the results of our simulations with experimental data reported earlier on ordering kinetics in FePt films. Figure 3 (a) shows the S -versus- t (number of pulses) dependence (circles) retrieved in Ref. [7] by detecting the increase X-ray diffraction from the formed $L1_0$ superstructure. Although the signal from the superstructure was observed after irradiation only, the extrapolation of the experimental curve into the time moment $t=0$ indicates the partial ordering $S(0)=0.47$ in an as-prepared Fe/Pt multilayer. This conclusion is consistent with other studies, where the formation of the partially ordered structure with S up to ~ 0.5 was observed in course of the multilayer film growth at elevated temperature of the substrate, e.g., $T=160^\circ\text{C}$ [3].

It is interesting to check if the experimental data $S-t$ presented in Fig. 3 (a) can be compatible to the results of solving numerically the Dienes equation [28] with taking into account the factor of $c_v(t)$ what we do in the paper. In the same plot we show theoretical dependences S -versus- t derived at $T=700^\circ\text{C}$ and different values of E – 2.7 eV, 2.56 eV and 2.45 eV, whereas the rest of parameters were retained to be fixed: $c_v(0)=c_{eq}(T=700^\circ\text{C})$, $S(0)=0.47$, $D_0=2.5 \times 10^{-6}$ m²/s, $L=10$ nm, and $E_v=1.53$ eV. As we see, the best

agreement between the modeling results and experiment occurs at $E=2.56$ eV. We note here that the most important parameter is the barrier $E_m=E-E_v$ for vacancy migration, which affects the ordering rate via the exponential factor in the Arrhenius law for the vacancy mobility D_m .

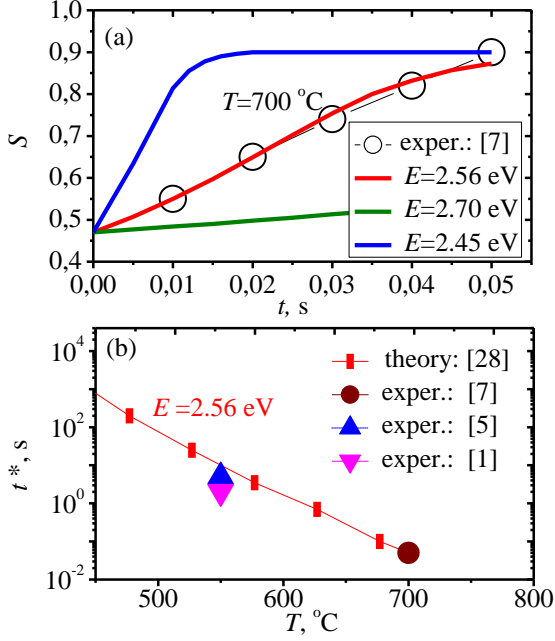


Fig.3. (a) Simulated S -versus- t dependence at $T=700$ °C for different E – 2.56 eV, 2.70 eV, and 2.45 eV. The simulation results were compared to the experimental S - t curve obtained (circles) in Ref. [7]. (b) Simulated timescale t^* on which the ordering occurs as a function of temperature T (solid curve). The symbols are the experimental data earlier reported.

We also compared the modeling results in terms of the temperature dependence of the characteristic timescale t^* , on which the ordering ($S \rightarrow 1$) occurs, with experimental data obtained in different studies [1, 5, 7] of the ordering kinetics in FePt multilayers. As illustrated in Fig. 3 (b), despite different experimental conditions and technological peculiarities of sample preparation, we find that the experimental data, that is, $t^* \sim 0.05$ s at $T=700$ °C [7] and $t^* \sim 10$ s at $T=550$ °C [1, 5], are compatible with the theoretical t^* -versus- T dependence derived at $E=2.56$ eV and $S(0)=0.47$. Note here that, at such time and temperature regimes, the ordering rate depends on $c_{eq}(T)$ but not $c_v(0)$.

D. Low-temperature ordering

Obviously, nonequilibrium vacancies, that can be injected into the alloy by quenching, should quickly migrate and annihilate at the boundaries of the alloy or crystallites at high T , so that the vacancy

concentration c_v will tend to the equilibrium $c_{eq}(T)$ if $t \gg \tau = L^2/D_m$. Formally, such a behavior is reflected in Eq. (5) [29], whose solution describes the temporal evolution of c_v . Therefore, if T is high enough, it is hard to expect the effect of the initial vacancy concentration $c_v(0)$ on the ordering kinetics. However, the factor of c_v becomes effective in the other limit, $t \ll \tau$. The relaxation time τ of nonequilibrium vacancies (and hence the ordering rate) can be increased by enlarging the sample or crystallites, which is actually not desirable in view of possible practical applications of such alloys [20, 23].

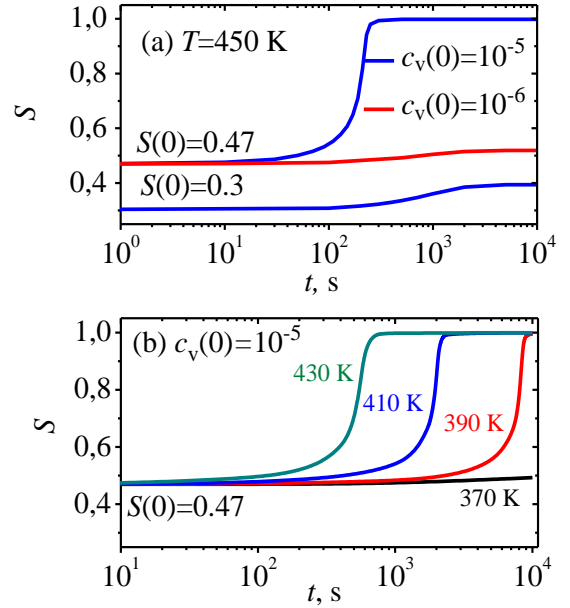


Fig.4. (a) S -versus- t at $T=450$ K, $c_v(0)=10^{-5}$ and 10^{-6} , $S(0)=0.3$ and 0.47 . (b) S -versus- t at $c_v(0)=10^{-5}$ and different values of T varied from 370 K to 430 K.

Another possibility for increasing τ is to lower T . By contrast, the usage of low-temperature standard annealing would be useful for improving the functional properties of the ordered alloys [3]. However, the lower T , the lower vacancy migration mobility D_m and thus the lower the ordering rate. Therefore, there is a competition between these two opposing factors in Eq. (4) which describes the relaxation of S by taking into account the factor of c_v .

Our simulations show that there is a region of low T , in which there can be the complete ordering ($S \rightarrow 1$) of the initially partially ordered [$S(0) > 0.3$] alloy [3] for $t < 10^4$ s provided that the initial vacancy concentration is not so small, $c_v(0) \geq 10^{-5}$. This is illustrated graphically in Fig. 4, where we show S -versus- t dependences simulated (a) at $T=450$ K, $c_v(0)=10^{-5}$ and 10^{-6} , and $S(0)=0.47$ and 0.3 as well as (b) at $c_v(0)=10^{-5}$ and T varied from 370 K to 430 K. We see that the factor of $c_v(0)$ is critical for effective

low-temperature ordering. For example, at $c_v(0)=10^{-6}$ and $T=450$ K the ordering does not practically occur for $t < 10^4$ s (Fig. 4, a). However, an increase of $c_v(0)$ to 10^{-5} at the same T provides $S \rightarrow 1$ for $t \sim 10^2$ s. As seen from plotting c_{eq} as a function of T (Fig. 2, c), the level of $c_v(0) \sim 10^{-5}$ in FePt is achievable at $T \sim 1500$ K. Such temperatures are still lower than $T_c=1600$ K at which the alloy becomes completely disordered ($S_{eq}=0$) in the equilibrium state.

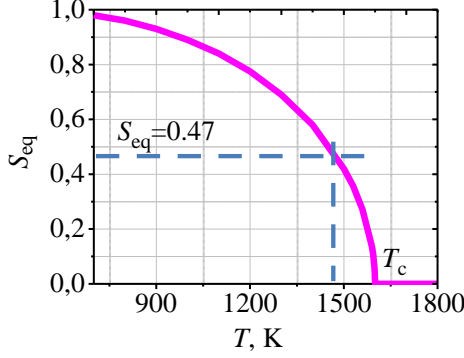


Fig.5. The order parameter S_{eq} at the equilibrium ($t \rightarrow \infty$) versus T . The S_{eq} level sufficient for effective low-temperature ordering (Fig. 4) is indicated.

Nevertheless, there are at least two questions at this point. One of them is how rapidly should the sample be quenched after heating up to the maximum temperature T_{max} close to T_c , in order to prevent thermalizing vacancies at a lower level of their concentration, as illustrated in Fig. 2 (c)? Another question is whether can the partial ordering $S(0) > 0.3$, which is sufficient for effective low-temperature ordering up to $S \rightarrow 1$ (Fig. 4, a), be conserved after quenching? Indeed, quenching from T_{max} close to T_c can reduce $S(0)$ to S_{eq} , which approaches zero at $T_{max} \rightarrow T_c$. The $S_{eq}(T)$ dependence, obtained by numerically solving Eq. (4), is shown in Fig. 5.

E. Injection of nonequilibrium vacancies

Both of the above issues can be solved by treating preliminarily the alloy with short-pulse laser irradiation. Figure 6 (a) shows the simulated temporal evolution of the temperature averaged across a film of FePt with thickness of $L=10$ nm on a glass substrate irradiated with a Gaussian laser pulse of duration of $\sigma=25$ ns. The $T(t)$ dependence was calculated according to the formula as follows [31]:

$$T(t) = T(0) + I \int_0^t q(u) g(t-u) du, \quad (10)$$

where $I = F(1 - \exp[-\delta L]) / \delta / L / (\rho c)_f = 409$ K/s, $F = 1.5 \times 10^{17}$ W/m³ is the power density absorbed by a sample, $L=10$ nm, $\delta=0.05$ nm⁻¹ is the coefficient of

light attenuation in a sample, which depends on the light wavelength, $\rho_f=15000$ kg/m³ is the density of an FePt film [8], $c_f=200$ J/kg/K is the specific heat capacity of an FePt film [8], $q(t) = \exp[-4 \ln 2 (t-t_0)^2 / \sigma^2]$ is the temporal evolution of pulse intensity, $g(t) = \exp(\gamma^2 t) \text{Erfc}(\gamma t^{1/2})$, $\gamma = (\rho c \lambda)_s^{1/2} / L / (\rho c)_f = 1.3$ ns^{-1/2} is the factor that reflects the substrate effect on film heating, $\rho_s=2300$ kg/m³ is the substrate density, $c_s=840$ J/kg/K is the specific heat capacity of the substrate, $\lambda_s=0.8$ W/m/K is the heat conductivity of the substrate (glass). The heating regime for an FePt sample on a glass substrate, illustrated in Fig. 6 (a), can be provided with a pulsed nanosecond laser with fluence of ~ 100 mJ/cm².

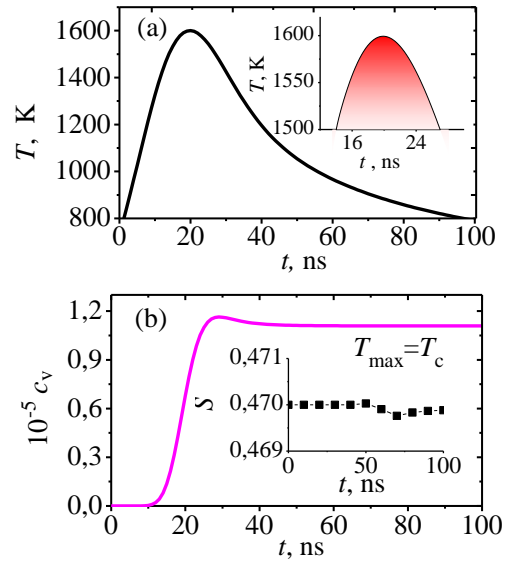


Fig.6. (a) Temporal profile of T in an FePt film provided by a laser pulse of the Gaussian shape of duration of $\sigma=25$ ns. (b) c_v -versus- t during the pulse of $\sigma=25$ ns duration, which heats the film up to $T_{max}=T_c$. The inset shows the S -versus- t evolution at $S(0)=0.47$ during the pulse.

Having simulated the $T(t)$ profile (Fig. 6, a), one may derive $c_v(t)$ under nonisothermal conditions by using Eq. (6). Figure 6 (b) shows changes in c_v during the pulse that heats the film up to $T_c=1600$ K. We find that it produces the vacancy concentration $c_v \approx 1.1 \times 10^{-5}$ which would be sufficient for effective low-temperature ordering (Fig. 4). Importantly, there is no a decrease in S during such short-pulse irradiation which heats the film even up to $T_{max}=T_c$, as shown in inset of Fig. 6 (b).

IV. CONCLUSIONS

Using the example of a practically important Fe-Pt alloy, it is theoretically shown that, due to

nonequilibrium vacancies artificially injected into the alloy, compositional ordering in this alloy becomes achievable at temperatures of ~ 450 K, which are significantly lower than the temperatures usually used in the technology of such functional alloys. The ordering kinetics was simulated on the basis of the chemical balance equation for order-disorder transformations proposed by Dienes [28]. Being rather phenomenological and not sensitive to neither the type of atomic lattice nor the kind of phase transformation (spinodal ordering [24] or nucleus growth [25]), the Dienes approach is relatively simple and universal to be potentially attractive for analyzing obtained experimental data. However, in its original form this approach does not take into account such a critical parameter as the vacancy concentration c_v in the alloy. To treat the effect of c_v , we have redefined the coefficients K_1 and K_2 in the Dienes equation [Eq. (1)], which characterize rates of the transformations. An experimental verification of the predictions reported here on low-temperature ordering after injecting nonequilibrium vacancies would be helpful for producing ordered alloys with good functional properties.

ACKNOWLEDGMENTS

Work was supported by RFBR (#20-02-00356).

REFERENCES

1. J.-Y. Chiou, H. W. Chang, C.-C. Chi, C.-H. Hsiao, and C. Ouyang, $L1_0$ FePt films with optimal (001) texture on amorphous SiO_2/Si substrates for high-density perpendicular magnetic recording media, *ACS Appl. Nano Mater.*, **2** (9), 5663–5673 (2019).
2. N. Y. Schmidt, S. Laureti, F. Radu, H. Ryll, C. Luo, F. d’Acapito, S. Tripathi, E. Goering, D. Weller, and M. Albrecht, Structural and magnetic properties of FePt-Tb alloy thin films, *Phys. Rev. B* **100**, 064428 (2019).
3. T. Shima, T. Moriguchi, S. Mitani, and K. Takanashi, Low-temperature fabrication of $L1_0$ ordered FePt alloy by alternate monatomic layer deposition, *Appl. Phys. Lett.* **80** (2), 288-290 (2002).
4. E. Yang, S. Ratanaphan, J.-G. Zhu, and D. E. Laughlin, Structure and magnetic properties of $L1_0$ -FePt thin films on TiN/RuAl underlayers, *J. Appl. Phys.* **109**, 07B770 (2011).
5. M. L. Yan, N. Powers, and D. J. Sellmyer, Highly oriented nonepitaxially grown $L1_0$ FePt films, *J. Appl. Phys.* **93**, 8292-8294 (2003).
6. C. Brombacher, C. Schubert, M. Daniel, A. Liebig, G. Beddies, T. Schumann, W. Skorupa, J. Donges, S. Häberlein, and M. Albrecht, Chemical ordering of FePt films using millisecond flash-lamp annealing, *J. Appl. Phys.* **111**, 023902 (2012).
7. Y. Inaba, G. B. Thompson, J. W. Harrell, T. Klemmer, and Y. Kubota, The FePt phase transformation in thin films using multiple laser pulsing, *J. Appl. Phys.* **107**, 053507 (2010).
8. J. Buschbeck, S. Fähler, M. Weisheit, K. Leistner, J. McCord, B. Rellinghaus, and L. Schultz, Thermodynamics and kinetics during pulsed laser annealing and patterning of FePt films, *J. Appl. Phys.* **100**, 123901 (2006).
9. G. H. Vineyard, Theory of order-disorder kinetics, *Phys. Rev.* **102** (4), 981-992 (1956).
10. K. Gschwend, H. Sato and R. Kikuchi, Kinetics of order-disorder transformations in alloys. II, *J. Chem. Phys.* **69** (11), 5006-5019 (1978).
11. R. Kozubski, M. Kozłowski, K. Zapala, V. Pierron-Bohnes, W. Pfeiler, M. Rennhofer, B. Sepiol, and G. Vogl, Atomic migration on ordering and diffusion in bulk and nanostructured FePt intermetallic, *J. Phase Equilibria. Diffus.* **26** (5), 482-486 (2005).
12. M. Leitner, D. Vogtenhuber, W. Pfeiler, W. Püschl, Monte-Carlo simulation of atom kinetics in intermetallics: Correcting the jump rates in Ni_3Al , *Intermetallics* **18**, 1091-1098 (2010).
13. P. Sowa, A. Biborski, M. Kozłowski, R. Kozubski, I. V. Belova, and G. E. Murch, Atomistic origin of the thermodynamic activation energy for self-diffusion and order-order relaxation in intermetallic compounds I: analytical approach, *Philos. Mag.* **97** (17), 1361-1374 (2017).
14. H.B. Luo, Q.M. Hu, J. Du, A.R. Yan, J.P. Liu, Thermal vacancy formation enthalpy of random solid solutions: The FePt case, *Comp. Mater. Sci.* **143**, 206–211 (2018).
15. J. J. Burton, Vacancy-formation entropy in cubic metals, *Phys. Rev. B* **5** (8), 2948-2957 (1972).
16. N. I. Polushkin, Chemical order relaxation in a substitutional solid alloy around the critical temperature, *Phys. Rev. B* **103** (10), 104207 (2021).
17. W. L. Bragg and E. J. Williams, The effect of thermal agitation on atomic arrangement in alloys, *Proc. Roy. Soc. A* **145** (855), 699-730 (1934).
18. F. C. Nix and V. Shockley, Order-disorder transformations in alloys, *Rev. Mod. Phys.* **10** (1), 1-71 (1938).
19. L. Scheuer, M. Ruhwedel, D. Karfaridis, I.G. Vasileiadis *et al.*, THz emission from Fe/Pt

- spintronic emitters with L1₀-FePt alloyed interface, *iScience* **25**, 104319 (2022).
20. B. Zhou, B. S. D. C. S. Varaprasad, C. Xu, M. -H. Huang, D. E. Laughlin and J. -G. Zhu, Fabrication of FePt/FePt-BN/FePt-SiO_x granular film for HAMR media on Corning Lotus™ NXT glass substrate, *IEEE Trans. Magn.* **58** (2), 1-5 (2022).
 21. W. Pei, D. Zhao, C. Wu, Z. Sun, C. Liu, X. Wang, J. Zheng, M. Yan, J. Wang, and Q. Wang, Direct Synthesis of L1₀-FePt Nanoparticles with High Coercivity via Pb Addition for Applications in Permanent Magnets and Catalysts, *ACS Appl. Nano Mater.* **3** (2), 1098–1103 (2020).
 22. F. M. Abel, V. Tzitzious, E. Devlin, S. Alhassan, D.J. Sellmyer, and G. C. Hadjipanayis, Enhancing the ordering and coercivity of L1₀ FePt nanostructures with Bismuth additives for applications ranging from permanent magnets to catalysts, *ACS Appl. Nano Mater.* **2** (5), 3146–3153 (2019).
 23. D. Weller, G. Parker, O. Mosendz, A. Lyberatos, D. Mitin, N. Y. Safonova, M. Albrecht, FePt heat assisted magnetic recording media, *J. Vac. Sci. & Techn. B* **34**, 060801 (2016).
 24. T. Mohri, First-principles calculations of spinodal ordering temperature and diffuse intensity scattering spectrum for Fe-Pt system, *J. Phase Equilibria. Diffus.*, **32** (6), 537-542 (2011).
 25. D. C. Berry and K. Barmak, Time-temperature-transformation diagrams for the A1 to L1₀ phase transformation in FePt and FeCuPt thin films, *J. Appl. Phys.* **101**, 014905 (2007).
 26. A. Kushida, K. Tanaka, and H. Numakura, Chemical Diffusion in L1₀-Ordered FePt, *Mater. Trans.* **44** (1), 59-62 (2003).
 27. O. Kubaschewski, Iron – Binary phase diagrams (Springer-Verlag, Germany, 1982).
 28. G. J. Dienes, Kinetics of order-disorder transformations, *Acta Metall.* **3**, 549-557 (1955).
 29. V. I. Boiko, B. S. Luk'anchuk, E. P. Tsarev, Generation and phase transitions in an ensemble of elastically interacting vacancies at laser heating of metals, In proceedings of Institute of General Physics of Russian Academy of Sciences, v. 30 (Laser generation of nonequilibrium defects in solid state), p. 6-82, "Nauka", Moscow (1991).
 30. P. G. Shewmon, Diffusion in solids (McGraw-Hill Book Company Inc., New-York, 1966).
 31. J. Trice, D. Thomas, C. Favazza, R. Sureshkumar, and R. Kalyanaraman, Pulsed-laser-induced dewetting in nanoscopic metal films: Theory and experiments, *Phys. Rev. B* **75**, 235439 (2007).